

Quasiparticle Interactions in Two-Dimensional Fluid ^3He Films Adsorbed on Graphite

C. P. Lusher, B. P. Cowan, and J. Saunders

*Department of Physics, Royal Holloway and Bedford New College, University of London,
Egham, Surrey, TW20 0EX, United Kingdom*

(Received 22 February 1991)

The nuclear magnetic susceptibility of ^3He adsorbed on the surface of graphite, plated with a monolayer of solid ^4He , has been measured at surface densities less than 0.055 \AA^{-2} and at temperatures down to 6 mK. A temperature-independent susceptibility is observed at low temperatures, which is strongly enhanced over the ideal-gas value, due to quasiparticle interactions. The inferred Landau-Fermi-liquid parameters allow a comparison with microscopic theories of interacting Fermi systems.

PACS numbers: 67.50.-b, 67.70.+n

The fluid phase of adsorbed ^3He is potentially an important and well characterized example of a low-dimensional system of highly correlated fermions. In this Letter we show that ^3He adsorbed on graphite plated with a single atomic layer of ^4He behaves as a two-dimensional Landau Fermi liquid, in which the interactions can be varied over a wide range and the crossover from degenerate to nondegenerate behavior can be clearly explored. We present the first measurements on two-dimensional ^3He to show a constant low-temperature nuclear magnetic susceptibility which is strongly enhanced by quasiparticle interactions above ideal-gas values. The Fermi-liquid parameters inferred from these measurements provide a test of microscopic models of interacting Fermi systems, such as the almost localized fermion model.

The two related systems that have received the most attention are ^3He adsorbed on exfoliated graphite [1] and ^3He - ^4He mixture films adsorbed on heterogeneous substrates [2,3]. In the mixture films the ^3He atoms reside near the surface of a ^4He film which coats the substrate, smoothing out effects of substrate heterogeneity. The interaction of the ^3He atoms with the ^4He film gives rise to a mass enhancement of the single ^3He "impurity" due to hydrodynamic backflow. In addition the ^3He atom has available excited states, at relatively low energy, associated with motion perpendicular to the surface. These states become populated therefore at relatively low coverages $\sim 0.03 \text{ \AA}^{-2}$, and need to be taken into account at temperatures above a few hundred millikelvin [2,4].

The system we have chosen to study is the second-layer fluid phase of ^3He on Grafoil [5]. Here the significantly higher fluid density of 0.055 \AA^{-2} is accessible before solidification commences [6,7] (the onset of promotion to the third layer occurs at 0.069 \AA^{-2}). At these higher fluid densities strong correlation effects are observable. The binding energy of the second-layer atoms is relatively large, ~ 25 K, and since the excitation of atoms out of this layer is negligible below 1 K the onset of degeneracy in the two-dimensional fluid can be investigated quantitatively. The more strongly bound first-layer submonolayer film also exhibits a fluid phase [1]. However, the range of

fluid densities is limited by a transition to a solid-fluid coexistence region [8,9] and, furthermore, in measurements of the nuclear magnetic susceptibility the fluid signal is masked by atoms localized by weak substrate inhomogeneity [8].

In order to study the magnetic properties of the second-layer fluid on graphite it was necessary to eliminate the large Curie law susceptibility originating from the solid ^3He first layer. This was done by preplating the graphite with a monolayer of ^4He atoms, which bind preferentially to the surface. A constant low-temperature susceptibility (characteristic of a 2D Fermi liquid) coming from the second-layer ^3He was then observed, which showed large enhancements above the ideal-gas value. The measurements were made using continuous-wave NMR with the cell and apparatus discussed in an earlier publication [8].

The surface area of the Grafoil sample was determined by locating monolayer completion of a pure ^3He film from the associated distinct cusp [8] in the spin-spin relaxation time T_2 . The surface density at this point was taken to be [10] 0.108 \AA^{-2} . In order to plate the surface with a monolayer of ^4He we added ^4He gas progressively to a sample of initially pure ^3He of surface density 0.013 \AA^{-2} . Between each coverage the sample was annealed at 15 K. The presence of localized ^3He in the first layer had the clear signature of a large temperature-dependent susceptibility at low temperatures, and the preferential promotion of the ^3He atoms to the second layer could clearly be seen through a reduction in this susceptibility. The final coverage of ^4He was slightly larger (by a few percent) than the known density of the ^4He first-layer solid layer at monolayer completion. The data shown in Fig. 1 at this ^3He coverage clearly demonstrate a constant low-temperature susceptibility arising from the degenerate fluid ^3He in the second layer. Higher second-layer densities were achieved by adding ^3He and annealing at 4 K. The measured fluid susceptibilities are shown in Fig. 1, where a correction to account for a residual small proportion of localized spins has been made for the higher fluid densities [11].

The enhancement of the $T=0$ susceptibility of an in-

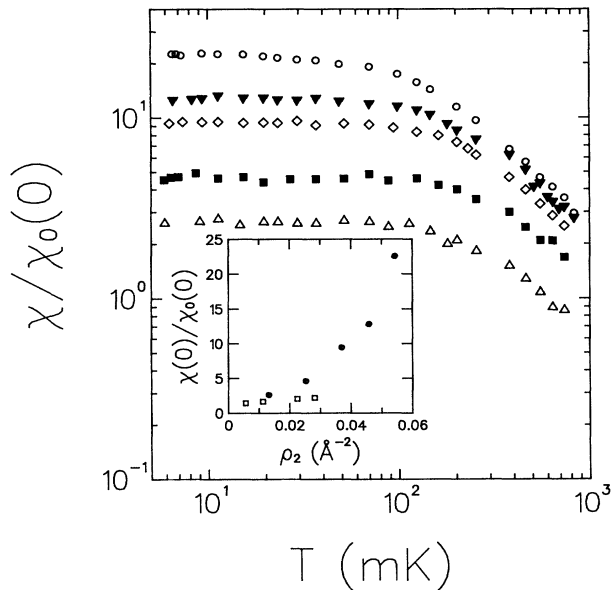


FIG. 1. Susceptibility normalized by zero-temperature ideal-gas susceptibility as a function of temperature for second-layer ${}^3\text{He}$ surface densities (\AA^{-2}) of 0.0132 (Δ), 0.0252 (\blacksquare), 0.0370 (\diamond), 0.0459 (\blacktriangledown), and 0.0543 (\circ). Inset: Coverage dependence of zero-temperature susceptibility enhancement: \bullet , this work; \square , mixture film, Ref. [3].

interacting Fermi liquid, $\chi(0)$, relative to an ideal Fermi gas of the same density, $\chi_0(0)$, is given by $\chi(0)/\chi_0(0) = (m^*/m)(1+F_0^q)^{-1}$, where m^* is the effective mass and F_0^q is a Landau parameter. Here $\chi_0(0) = C/T_F$ (in 2D), where C is the Curie constant and T_F the Fermi temperature of the ideal gas. Since both C and T_F are proportional to surface density in 2D, $\chi_0(0)$ is independent of coverage. The Curie constant at each coverage was determined from the limiting value of χT at high temperatures; the values obtained in the fluid phase and at higher coverages of 0.066 and 0.068 \AA^{-2} , for which the second layer was completely solid, were consistent and proportional to surface density as expected.

The coverage dependence of the observed susceptibility enhancements are compared in Fig. 1 (inset) with representative values for mixture films [3]. In the latter case the enhancement is observed to increase with decreasing film thickness; such an effect has been calculated to arise [12] from the influence of the ${}^4\text{He}$ background on the two-body ${}^3\text{He}$ atom correlations, higher-order correlations being neglected. In addition the hydrodynamic effective mass has been calculated to depend on the structure of the background ${}^4\text{He}$ film [13]. In contrast, in our experiments the ${}^3\text{He}$ atoms are tightly bound to an essentially incompressible ${}^4\text{He}$ solid film and the effective-mass enhancement arises from direct interatomic interactions. At a given surface density these films show larger susceptibility enhancements than the mixture films. It would therefore appear that, in general, interactions in these

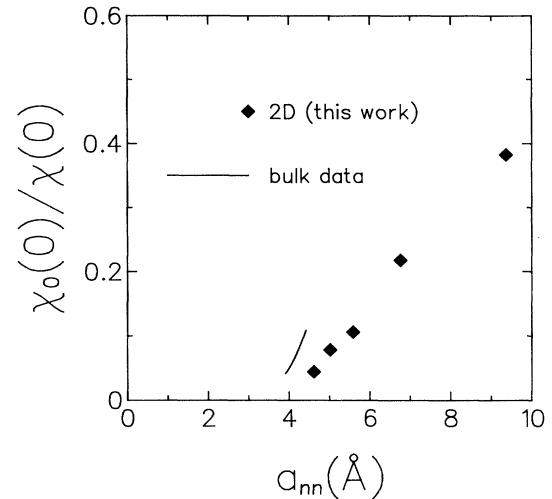


FIG. 2. Comparison of inverse susceptibility enhancement as a function of interatomic separation in 2D and bulk (Ref. [17]).

two-dimensional films are influenced by the details of the bound states along the surface normal, which depend on the particular adsorbate used. The higher densities that can be explored for ${}^3\text{He}$ on graphite, without exciting surface-normal states above the ground state, allow the observation of susceptibility enhancements an order of magnitude greater than in the mixture films.

A comparison of interactions in 2D with those in bulk can be made by examining the dependence of the inverse susceptibility enhancement on interatomic spacing a_{nn} (Fig. 2), as has been done for the effective mass [14]. At the maximum achievable 2D density, for which a_{nn} is approximately that in bulk liquid at zero pressure, it is seen that the susceptibility enhancement is much greater in 2D and approximately equal to that of bulk liquid on the melting curve. Furthermore, the figure clearly illustrates the wider range of interparticle spacing that can be explored in 2D.

The Landau parameter F_0^q may be inferred from the measured susceptibility enhancement using the effective-mass data of Greywall [14]. These latter results were obtained in heat-capacity measurements on pure ${}^3\text{He}$ films, i.e., with a solid ${}^3\text{He}$ first layer; the isotopic composition of the first layer does not appear to affect the properties of the second layer significantly [15]. The relative dependence of the two interaction parameters F_0^q and m^*/m then provide a test of microscopic models of the interacting Fermi system, since both quantities in general depend on the same parameters of the microscopic model. The simplest example of this is calculations in the low-density limit, including only two-body interactions, in which all Landau parameters are given in terms of a single interaction parameter [16].

The experimental relative dependence of $1+F_0^q$ and m^*/m for 2D and bulk ${}^3\text{He}$ [17] is shown in Fig. 3. The inset of this figure shows the dependence of the suscepti-

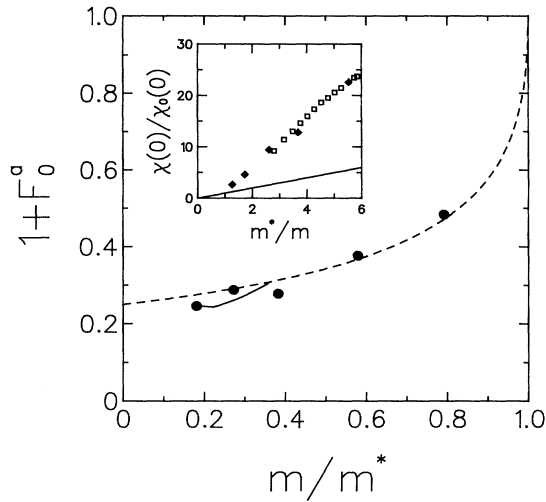


FIG. 3. Relative dependence of $1+F_0^g$ and m/m^* : ●, this work; —, values for bulk from Ref. [17]; ---, prediction of almost localized fermion model (see text). Inset: The dependence of the measured susceptibility enhancement on m^*/m : ◆, this work; □, bulk data. The straight line is $\chi/\chi_0 = m^*/m$.

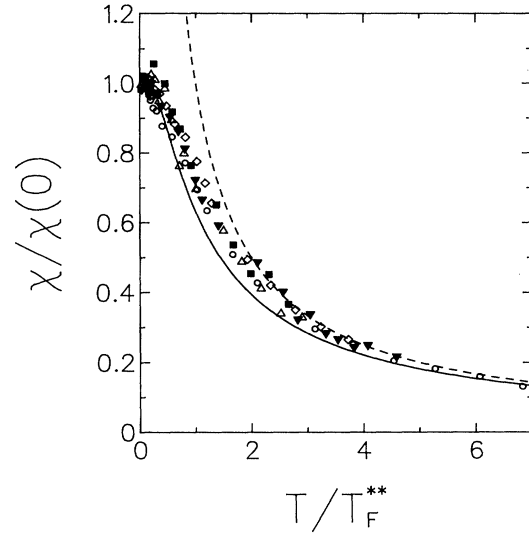


FIG. 4. Dependence of reduced susceptibility on reduced temperature for data of Fig. 1. Solid curve: modified Fermi-gas expression. Dashed curve: Curie law.

bility enhancement on the effective mass. The straight line in the inset is the susceptibility enhancement that would be expected in the absence of spin-dependent quasiparticle interactions ($\chi/\chi_0 = m^*/m$).

The similarity of the bulk and 2D results is striking. In particular, in the strongly interacting limit the observed value for $1+F_0^g$ is seen to plateau around 0.25. This result emerges naturally from the almost localized fermion model [18,19], which treats ^3He in terms of a Hubbard model with a half-filled band [20,21]. The Fermi-liquid parameters are given in terms of a normalized on-site interaction potential $I=U/U_c$. It is found that $m^*/m = (1-I^2)^{-1}$ and $F_0^g = -p[1-1/(1+I)^2]$. Here p depends on the precise form of the density of states but is approximately 1 for a symmetric band [20]. Thus the effective mass diverges as $I \rightarrow 1$ but F_0^g saturates at $-0.75p$. The theoretical curve for $p=1$ is shown in Fig. 3, and agrees well with both the 2D and bulk data. This suggests that the model contains the essential physics describing the static properties of ^3He . In both 2D and 3D the spin-dependent interactions are weakly density dependent at the highest densities and the large increases in susceptibility arise from increases in the effective mass rather than any incipient ferromagnetic tendency [19].

In the low-density limit the model gives $F_0^g \propto -(1-m/m^*)$ and this result is also found in the binary interaction model [22], in both 3D and 2D, with a different constant of proportionality in each case. Clearly, $F_0^g \rightarrow 0$ and $m^*/m \rightarrow 1$ in the weakly interacting limit. Unlike bulk ^3He the low-density limit can be explored in 2D ^3He and more measurements in this region would be valuable [23]. The clear advantage of ^3He as a model Fermi sys-

tem is that the effective mass appears to be a direct measure of the interatomic interactions relevant to the static properties.

Versions of the induced interaction model [24] have also been shown to account well for the static properties of bulk ^3He , but here a knowledge of F_0^g is required before a prediction of the density dependence of F_0^g and F_1^g can be made.

We now discuss the measured temperature dependence of the nuclear magnetic susceptibility through the onset of degeneracy. In Fig. 4 we represent the normalized 2D susceptibility data $\chi(T)/\chi(0)$ at all surface densities as a function of the reduced temperature T/T_F^{**} , where at each coverage $\chi(0)$ is the susceptibility at $T=0$ and $T_F^{**} = C/\chi(0)$. Within the scatter it is apparent that the results can be successfully reduced in this way onto a single curve by the scaling parameter $\chi(0)$, which itself increases by more than an order of magnitude over the studied coverage range. The dashed line shows the Curie law, and the solid line the ideal-Fermi-gas susceptibility, modified by replacing the Fermi temperature by T_F^{**} , giving [25] $\chi/\chi(0) = 1 - \exp(-T_F^{**}/T)$. Similar universal behavior was also seen in bulk liquid [26], where an initial T^2 correction to the zero-temperature susceptibility due to spin fluctuations has been calculated using the paramagnon model [27]. This scales with $\chi(0)$ and is in good agreement with experiment. However, the calculation of the spin fluctuation contribution to thermodynamic quantities [28] appears to be technically problematic in 2D [29].

Earlier theories of the magnetic susceptibility of 2D ^3He at finite temperatures use the method of statistical

quasiparticles with a simplified binary interaction [30, 31]. These theories, which only apply at low densities, do not fit the observed $\chi(T)$. In particular, they are not consistent with the scaling properties discussed above.

The fluid ^3He film adsorbed on graphite provides a clean example of a two-dimensional Fermi system for which the density can be varied from the weakly interacting to the strongly correlated limit. The thermodynamic properties of such films measured so far (heat capacity and nuclear magnetic susceptibility) are consistent with those of a Landau Fermi liquid and are found to be in agreement with the predictions of the almost localized fermion model.

-
- [1] M. Bretz, J. G. Dash, D. C. Hickernell, E. O. McClean, and O. E. Vilches, *Phys. Rev. A* **8**, 1589 (1973).
- [2] M. J. Dipirro and F. M. Gasparini, *Phys. Rev. Lett.* **44**, 269 (1980).
- [3] J. M. Valles, R. H. Higley, B. R. Johnson, and R. B. Hallock, *Phys. Rev. Lett.* **60**, 428 (1988).
- [4] R. H. Higley, D. T. Sprague, and R. B. Hallock, *Phys. Rev. Lett.* **63**, 2570 (1990).
- [5] Grafoil is a product of Union Carbide.
- [6] D. S. Greywall and P. A. Busch, *Phys. Rev. Lett.* **62**, 1868 (1989).
- [7] C. P. Lusher, J. Saunders, and B. P. Cowan (to be published).
- [8] J. Saunders, C. P. Lusher, and B. P. Cowan, *Phys. Rev. Lett.* **64**, 2523 (1990).
- [9] D. S. Greywall and P. A. Busch, *Phys. Rev. Lett.* **65**, 2788 (1990).
- [10] R. Feile, H. Wiechert, and H. J. Lauter, *Phys. Rev. B* **25**, 3410 (1982).
- [11] This number of localized spins was determined from the intercept χT ($T=0$) determined by fitting χT against T and corresponded to at most 1% of the total ^3He coverage.
- [12] E. Krotscheck, M. Saarela, and J. L. Epstein, *Phys. Rev. Lett.* **61**, 1728 (1988).
- [13] J. L. Epstein, E. Krotscheck, and M. Saarela, *Phys. Rev. Lett.* **64**, 427 (1990).
- [14] D. S. Greywall, *Phys. Rev. B* **41**, 1842 (1990). We assume $a_{nn} = 1.122/\rho^{1/3}$ in bulk (fcc lattice) and $1.075/\rho^{1/2}$ in 2D (triangular lattice), where ρ is the appropriate number density.
- [15] Our measurements of the coverages at which the second layer solidifies and promotion to the third layer occurs (Ref. [7]) on ^4He -preplated graphite are in good agreement with those of Ref. [14]. We also note that the heat-capacity data in the fluid phases of both first and second layer are in good agreement [Ref. [14] and D. S. Greywall and P. A. Busch, *Phys. Rev. Lett.* **65**, 64 (1990)].
- [16] A. A. Abrikosov and I. M. Khalatnikov, *Rep. Prog. Phys.* **22**, 329 (1959).
- [17] Bulk ^3He Fermi-liquid parameters tabulated in D. Vollhardt and P. Wolfe, *The Superfluid Phases of ^3He* (Taylor & Francis, London, 1990), p. 31.
- [18] W. F. Brinkman and T. M. Rice, *Phys. Rev. B* **2**, 4302 (1970).
- [19] P. W. Anderson and W. F. Brinkman, in *The Physics of Liquid and Solid Helium*, edited by K. H. Bennemann and J. B. Ketterson (Wiley, New York, 1978).
- [20] D. Vollhardt, *Rev. Mod. Phys.* **56**, 99 (1984).
- [21] The case of less than half filling has been addressed by D. Vollhardt, P. Wolfe, and P. W. Anderson, *Phys. Rev. B* **35**, 6703 (1987).
- [22] Abrikosov and Khalatnikov (Ref. [16]); B. P. Cowan (unpublished).
- [23] A limit on the hydrodynamic effective-mass enhancement due to the ^4He first layer may be obtained from Fig. 3 (inset); an extrapolated linear fit to the 2D data intersects $\chi/\chi_0 = m^*/m$ (i.e., $F\beta=0$) at $m^*/m = 0.9 \pm 0.2$.
- [24] K. S. Bedell and T. L. Ainsworth, *Phys. Lett.* **102A**, 49 (1984). A review of models of ^3He from fully microscopic to semiphenomenological may be found in Ref. [17].
- [25] This is equivalent to the molecular-field phenomenology suggested for bulk ^3He by L. Goldstein, *Phys. Rev.* **96**, 1455 (1954).
- [26] H. Ramm, P. Pedroni, J. R. Thompson, and H. Meyer, *J. Low Temp. Phys.* **2**, 539 (1970).
- [27] M. T. Beal-Monod, S. K. Ma, and D. Fredkin, *Phys. Rev. Lett.* **20**, 929 (1968).
- [28] For a recent view on bulk ^3He see D. Coffey and C. J. Pethick, *Phys. Rev. B* **37**, 1647 (1988), and references therein.
- [29] A. Theumann and M. T. Beal-Monod, *Phys. Rev. B* **29**, 2567 (1984).
- [30] S. M. Havens-Sacco and A. Widom, *J. Low Temp. Phys.* **40**, 357 (1980).
- [31] M. B. Vetrovec and H. T. Diaz, *J. Low Temp. Phys.* **69**, 209 (1987).